Talanta 126 (2014) 116–121

Contents lists available at ScienceDirect

Talanta

journal homepage: www.elsevier.com/locate/talanta

# Molecular interaction study of flavonoid derivative 3d with human serum albumin using multispectroscopic and molecular modeling approach

Juntong Wei [a,b,c,1], Feng Jin [b,d,1], Qin Wu [a,b,c], Yuyang Jiang [b,e], Dan Gao [b,c,*], Hongxia Liu [b,c,*]

[a] Department of Chemistry, Tsinghua University, Beijing 100084, China
[b] State Key Laboratory Breeding Base-Shenzhen Key Laboratory of Chemical Biology, Graduate School at Shenzhen, Tsinghua University, Shenzhen 518055, China
[c] Key Laboratory of Metabolomics at Shenzhen, Shenzhen 518055, China
[d] Neptunus Pharmaceutical Technology Center, Shenzhen 518057, China
[e] School of Medicine, Tsinghua University, Beijing 100084, China

ARTICLE INFO

*Article history:*
Received 19 November 2013
Received in revised form
15 March 2014
Accepted 18 March 2014
Available online 24 March 2014

*Keywords:*
Human serum albumin (HSA)
Spectrum
Molecular docking
Flavonoid derivative

ABSTRACT

Human serum albumin (HSA) has been developed as a model protein to study drug–protein interaction. In the present work, the interaction between our synthesized flavonoid derivative 3d (possessing potent antitumor activity against HepG2 cells) and HSA was investigated using fluorescence spectroscopy, circular dichroism spectroscopy, UV–vis spectroscopy and molecular modeling approach. Fluorescence spectroscopy showed that the fluorescence of HSA can be quenched remarkably by 3d under physiological condition with a slight shift of maximum fluorescence emission bands from 360 nm to 363 nm. Calculated results from Stern–Volmer equation and modified Stern–Volmer equation indicated that the fluorescence was quenched by static quenching processing with association constant $5.26 \pm 0.04 \times 10^4$ L mol$^{-1}$ at 298 K. After comprehensive consideration of the free energy change $\Delta G$, enthalpy change $\Delta H$ and entropy change $\Delta S$, electrostatic interactions were confirmed as the main factor that participate in stabilizing the 3d–HSA complex. Both dichroism spectroscopy and UV–vis spectroscopy indicated conformational change of HSA after binding to 3d. Moreover, the structure of HSA was loosened and the percentage of α-helix decreased with increasing concentration of 3d. Molecular modeling results demonstrated that 3d could bind to HSA well into subdomain IIA, which is related to its capability of deposition and delivery. Three cation–π interactions and three hydrogen bonds occurred between 3d and amino acid residuals ARG218, ARG222 and LYS199. In conclusion, flavonoid derivative 3d can bind to HSA with noncovalent bond in a relatively stable way, so it can be delivered by HSA in a circulatory system.



## 1. Introduction

Recently, the interaction between macromolecules such as protein and drugs has attracted increasing interest [1–4]. Serum albumins, the major transport protein in the blood circulatory system (accounting about half of the proteins in human blood), act as the transportation and disposition factor of various ligands, such as dyes, fatty acids, and drugs [5,6]. Human serum albumin (HSA) is the most abundant globular protein existing in plasma. It is made up of 585 amino acids and its polypeptide chain folds into a heart-shaped molecule. Its three dimensional (3D) structure was studied through X-ray crystallographic measurement [7]. 3D crystal structure shows that HSA consists of three homologous domains (namely I, II, and III): I (residuals 1–195), II (196–383) and III (384–585) and each domain has two subdomains (denoted by A and B) [8,9]. The main role of HSA is to maintain the blood pH and colloid osmotic blood pressure. Moreover, HSA can bind to various ligands (endogenous and exogenous), such as lipids, amino acids, nutrients, metal ions, drugs etc. [10–12]. Due to this capability, HSA is known to play an important role in transport and disposition of drugs. After entering the circulatory system (oral administration or injection), drugs bind to HSA more or less. It is easy to understand that binding affects pharmacokinetics and pharmacodynamics of drugs as it can prolong the action time from being metabolized [13]. Moreover, drug–HSA complex blocks drugs from penetrating blood capillary walls, blood–brain barrier and

* Corresponding authors at: State Key Laboratory Breeding Base-Shenzhen Key Laboratory of Chemical Biology, Graduate School at Shenzhen, Tsinghua University, Shenzhen 518055, China. Tel. /fax: +86 755 26036035.
*E-mail addresses:* gao.dan@sz.tsinghua.edu.cn (D. Gao), liuhx@sz.tsinghua.edu.cn (H. Liu).
[1] These authors contributed equally to this work.

http://dx.doi.org/10.1016/j.talanta.2014.03.046
0039-9140/

glomerulus. Therefore, the binding force cannot be too strong or too weak [12], for that if it is too strong, drugs cannot dissociate from HSA smoothly, resulting in low concentration of free drugs in plasma. While if it is too weak, patients have to keep taking in drugs to hold the concentration because its half-time is too short. Therefore, it is necessary to evaluate the binding affinity of lead compounds to HSA during the development of new drugs at an early stage.

Flavonoids containing the same skeleton of two aromatic rings linked by an oxygenated heterocycle are a huge family including flavones, flavonols, iso-flavones, anthocyanidins, anthocyanins, proanthocyanidins and catechins [14]. In the past two decades, they are considerably preferred more by researchers due to their diversity in nature and their biological effects and pharmacological activities, such as antitumor, anti-inflammatory, antiviral and cardio-protective properties [15–22]. Among these properties, the antitumor activity has attracted increasing interest in the development of flavonoids and their derivatives as new drugs. Researchers have already known that flavonoids from vegetables and fruits can reduce the risk of cancer [17,23]. This may be resulted from their ability of antioxidant activity because they could obliterate free radicals or be beneficial to this procedure [24]. In our previous work, a synthesized flavonoids derivative, 1-(3-chloro-4-(6-ethyl-4-oxo-4H-chromen-2-yl)phenyl)-3-(4-chloro-phenyl)urea (3d) (Fig. 1), possessed potential antitumor activity against HepG2 cells, while low toxicity against normal cells HL7702 and QSG7701. The antitumor mechanism had been investigated by conventional molecular biological methods and metabolomics approaches [25]. In light of 3d had the potential for further drug development, we further investigated the interaction between 3d and HSA to better understand the transport and distribution of 3d in blood.

To date, plenty of techniques have been applied to investigate the interaction of small molecules with protein, such as nuclear magnetic resonance (NMR) [2], fluorescence [26], UV–vis, circular dichroism (CD) [9] and Fourier transform infrared spectroscopy (FTIR) [8]. As time goes on, some methods also have been introduced such as mass spectrometry [27,28], capillary electrophoresis [29–31], high-performance liquid chromatography (HPLC) [32], surface-enhanced Raman scattering [33], electrochemistry methods [34] and molecular modeling [8,35] to elucidate the binding character. In this paper, the interaction of 3d with HSA was investigated using fluorescence spectroscopy, CD, UV–vis and molecular modeling methods. We chose the first three techniques because of their easy accessibility, sensitivity and abundant theoretical foundation. As to molecular modeling, it is viewed as the most useful tool to simulate conformation under the situation of no real cocrystallization. The aim of our study is to explore the binding mechanism of 3d to HSA and the effect of the complexation on the protein structure in detail by multispectroscopic methods. We hope this study can provide significant insight into the theoretical basis for pharmacology.

## 2. Material and methods

### 2.1. Reagents and materials

Human serum albumin (99%), Tris-base, $NaH_2PO_4$, $Na_2HPO_4$ and ammonium acetate (analytical grade) were purchased from Sigma-Aldrich (St. Louis, MO, USA). Acetonitrile (HPLC grade) was supplied by Merck (Darmstadt, Germany). Water used throughout this experiment was prepared by Milli-Q water purification system (Millipore, USA). Other reagents used were of analytical grade. The pH of 10 mM Tris–HCl buffer and 100 mM phosphate buffer were adjusted to 7.4 using hydrochloric acid and phosphoric acid respectively.

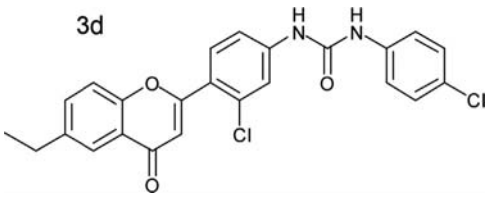


**Fig. 1.** Molecule structure of 3d.

### 2.2. Fluorescence spectroscopy

Fluorescence spectra were performed on a Fluorolog-3 fluorescence spectrophotometer (HORIBA JobinYvon, France) using a 1.0 cm quartz cell equipped with a thermostatic bath. The excitation wavelength was 280 nm while the emission spectra were recorded from 300 nm to 450 nm. Both the excitation and emission slit widths were set at 5 nm. The scan speed was 600 nm $min^{-1}$. HSA was dissolved in 10 mM Tris–HCl solution to obtain the protein concentration of 2.5 μM, with physiological pH 7.4. Titrate HSA with the prepared compound 3d to make sure that its final concentration ranged from 0 to 25 μM. Because the drug concentration of stock solution was far greater than HSA, the titration of drug can hardly change the final concentration of HSA. In order to let solution reach the setting temperature, data were collected after 3 min balance time when the quartz cell was placed in the thermostatic bath. The fluorescence emission spectra were recorded at 288 K, 298 K and 310 K, respectively. The appropriate blank corresponding to the buffer solution was subtracted to correct the background of fluorescence. The association constants of the HSA–3d system were calculated by the fluorescence data.

### 2.3. Circular dichroism (CD) spectroscopy

CD spectra were measured using a J-815 spectrometer (JASCO, Japan) with a 0.1 cm quartz cell. HSA was dissolved in 100 mM phosphate buffer (pH 7.4) as mentioned above and the signal was recorded at room temperature in the presence and absence of drugs from 200 nm to 250 nm at a scan speed of 200 nm $min^{-1}$. The concentration of HSA was 5 μM and drugs were dissolved in DMSO with the concentration of 10 mM. The molar ratios of drugs to HSA were varied as 0:1, 1:1, 2:1. Each of the CD spectra was an average of three times scanning after subtracting background value of phosphate buffer. All results were recorded as CD ellipticity in mdeg.

### 2.4. UV–vis absorption spectroscopy

UV–vis absorption spectra were measured on a Beckman Coulter DU-800 spectrophotometer (USA) at room temperature in 1.0 cm path length. The UV–vis absorption spectra of HSA in the present and absence of 3d were recorded in the range of 190–320 nm. The final concentrations of drugs used for absorption spectra changed from 0 to 25 μM, while the concentration of HSA was fixed at 2.5 μM.

### 2.5. Molecular modeling

Molecular docking was applied to simulate the binding conformations between 3d and HSA. X-ray crystal structure of the ligand bound to specific target protein provides accurate interactions between the ligand and the protein, including optimization of protein conformations and ligand position, orientation and active binding site, which makes it a potent tool for molecular modeling. In our study, the crystal structure of HSA (PDB ID: 2BXD) was downloaded from Protein Data Bank (PDB) based on high structure similarity between 3d and warfarin (an approved drug) [36], and the three dimensional structure of 3d was built

using Discovery Studio.3.1/CDOCK protocol (Accelrys Software Inc.). The processing of molecular docking was as follows: firstly, water crystallization was removed from the X-ray crystal structure of HSA; secondly, binding domain of warfarin was defined as the candidate binding sphere, then small molecular ligand warfarin was removed from the defined sphere, and HSA crystal structure (2BXD) was simulated with CHARMm force flied as the receptor; thirdly, 3d was applied by CHARMm force field, then was selected as the ligand. Finally, 3d was docked into the defined sphere. The possible conformation could be calculated and evaluated according to CDOCKER energy, and the top rank conformation was selected for further analysis.

## 3. Results and discussion

### 3.1. Fluorescence spectra analysis

In recent years, fluorescence spectroscopy has been widely used as a powerful tool for the study of interaction between biomolecules and ligands since it can provide significant parameters such as binding constant, binding sites, binding forces, interaction distance, and so on [37]. Due to its high sensitivity and non-intrusive measurement, fluorescence spectroscopy is highly appropriate for low concentration detection under physiological conditions. Generally, the emission fluorescence of HSA is mainly derived from the residues of tryptophan, tyrosine and phenylalanine. In fact, people usually take the fluorescence of tryptophan residues as the inherent fluorescence of HSA because phenylalanine has a relatively low quantum yield and the fluorescence of tyrosine is almost completely quenched if it is ionized or present near to an amino group, a carboxyl group or a tryptophan [38].

Fig. 2A shows the fluorescence quenching spectra of HSA induced by different concentrations of 3d in Tris–HCl solution with pH 7.4 at the excitation wavelength of 280 nm. It is obvious that the fluorescence intensity of HSA gradually decreased along with increasing $C_{drug}/C_{HSA}$ from 1 to 10 and the maximum fluorescence emission bands had a red-shift from 360 nm to 363 nm. It indicated that 3d could interact with HSA and quench its intrinsic fluorescence. Protein fluorescence is sensitive to microenvironment and its structure. As we know, the fluorescence emission wavelength of protein in polar solvent is longer than that in nonpolar solvent. In other words, it will result in red-shift with the increase of solvent polarity. The red-shift of the maximum fluorescence emission indicated that the microenvironment of tryptophan residue in HSA was changed, leading to an increase of hydrophilicity in the vicinity of this residue [39].

Fluorescence quenching mainly takes place by two different mechanisms, namely dynamic quenching and static quenching. In order to clarify the quenching mechanism of 3d–HSA system, the fluorescence spectra data were analyzed by the following Stern–Volmer equation to calculate the quenching constant $K_{SV}$:

$$\frac{F_0}{F} = 1 + K_q \tau_0 [Q] = 1 + K_{SV}[Q] \quad (1)$$

where $F_0$ and $F$ are the fluorescence intensities of HSA in the absence and presence of different concentrations of 3d, respectively. $K_q$ is bimolecular quenching rate constant, $\tau_0$ is the average lifetime of the fluorophore before addition of drugs (the HSA fluorophore lifetime is approximately $10^{-8}$ s); [Q] is the concentration of quencher (3d). In order to find out which mechanism plays the dominant role in this quenching process, the fluorescence intensities of 3d–HSA system analyzed by plotting $F_0/F$ versus [Q] at three different temperatures (288 K, 298 K and 310 K) are shown in Fig. 2B, and the calculated $K_{sv}$ values are listed in Table 1.

As shown in Fig. 2B, the regression lines under each detection temperature reveal quite a good linear relationship and their slope ($K_{sv}$) decreases from $5 \pm 0.05 \times 10^4$ to $3.57 \pm 0.03 \times 10^4$ L mol$^{-1}$ when the temperature rises from 288 K to 310 K. Generally, dynamic quenching and static quenching can be distinguished

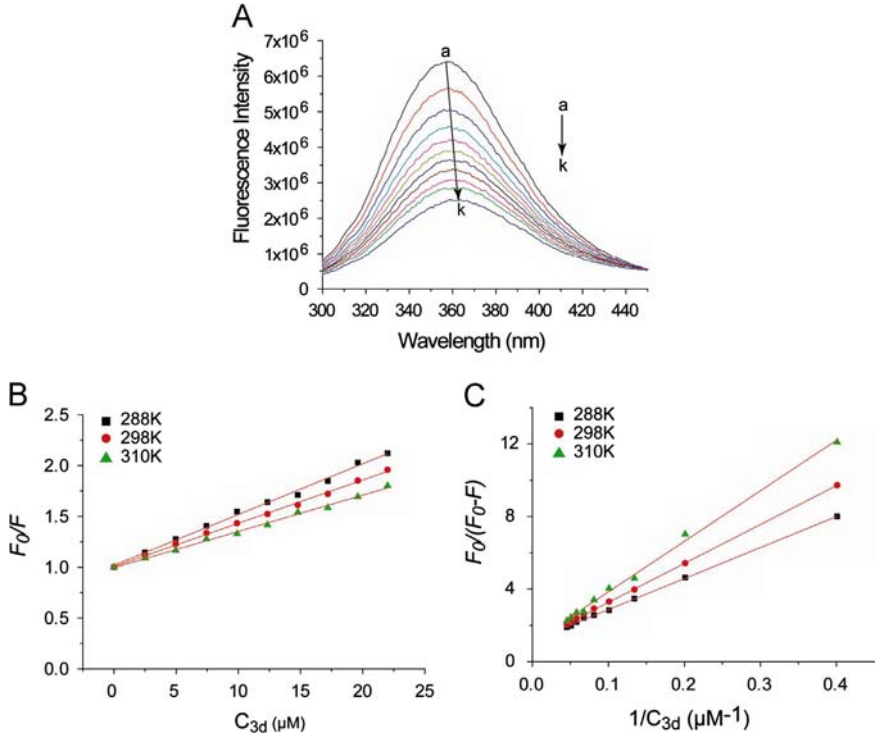


**Fig. 2.** (A) Fluorescence quenching curves of HSA induced by different concentrations of 3d in 10 mM Tris–HCl buffer, pH 7.4 at 298 K upon excitation at 280 nm and slit width of 5 nm. The concentration of HSA was 2.5 μM, whereas 3d concentrations were 0 – 25.0 μM at regular increments of 2.5 μM from top to bottom (a–k). (B) Stern–Volmer plot for fluorescence quenching data of HSA–3d system at three different temperatures (288 K, 298 K and 310 K). (C) Modified Stern–Volmer plot for fluorescence quenching data of HSA–3d system at three different temperatures as mentioned in B.

**Table 1**
The quenching constants ($K_{SV}$), association constants ($K_a$) and relative thermodynamic parameters of the HSA–3d system at different temperatures.

| $T$ (K) | $K_{SV}$ ($\times 10^4$ L mol$^{-1}$) | $R^{sv}$ | $K_a$ ($\times 10^4$ L mol$^{-1}$) | $R^a$ | $\Delta S$ (J mol$^{-1}$ K$^{-1}$) | $\Delta H$ (J mol$^{-1}$) | $\Delta G$ (J mol$^{-1}$ K$^{-1}$) | $R^b$ |
|---|---|---|---|---|---|---|---|---|
| 288 | $5 \pm 0.05$ | 0.9946 | $6.8 \pm 0.04$ | 0.9992 | 24.6232 | −19568.4 | −26659.9 | 0.9998 |
| 298 | $4.26 \pm 0.05$ | 0.9979 | $5.26 \pm 0.04$ | 0.9997 | | | −26906.1 | |
| 310 | $3.57 \pm 0.03$ | 0.9957 | $3.81 \pm 0.02$ | 0.9996 | | | −27201.6 | |

sv, a, and b represent the correlation coefficient for Stern–Volmer plot, $K_a$ and the van't Hoff plot, respectively.

by different $K_{sv}$ at different temperatures. As to dynamic quenching, the rise of temperature will increase the number of effective collision, which promotes the quenching process, leading to the increase of $K_{sv}$. On the other hand, higher temperature will decrease the stability of drug–HSA complex, inducing the decrease of $K_{sv}$. Hence the decrease of $K_{sv}$ in this experiment indicated that the fluorescence quenching came out of the formation of 3d–HSA complex rather than dynamic collision, that is to say, 3d bound to HSA. Table 1 gathers all the calculated $K_{sv}$ at each temperature.

The modified Stern–Volmer equation is used to achieve the association constant ($K_a$)

$$\frac{F_0}{F_0-F}=\frac{1}{fK_a}\frac{1}{[Q]}+\frac{1}{f} \quad (2)$$

where $f$ is the fraction of accessible fluorescence, $K_a$ is an effective quenching constant and here it can be viewed as equal to association constant in our quencher–acceptor system [40,41]. Fig. 2C shows a plot of $F_0/(F_0-F)$ against $1/([Q])$ and corresponding results are shown in Table 1. It can be seen that a good linear relationship was matched too, indicating that 3d interacts with HSA in a one-to-one ratio. The calculated association constants between 3d and HSA are all in the order of magnitude larger than $10^4$ M$^{-1}$. This result was in accordance with plenty of earlier reports, and such value of $K_a$ was considered to be good for the drug to diffuse from circulatory system to its target sites [10]. Moreover, the value of $K_a$ decreased as the temperature rose, which coincided with the change of $K_{sv}$ and supported the static quenching mechanism for 3d–HSA system. This information suggested that 3d and HSA have a noncovalent binding with moderate affinity so that 3d can be carried by HSA in the circulatory system and transferred to target tissue.

Since 3d and HSA have noncovalent interactions, we can move toward to determine which force plays the dominant role in that process. As is well known, weak interactions include hydrogen bonds, Van der Waals interaction, electrostatic interaction, hydrophobic force, etc. [42]. In this research, the type of weak interactions can be determined by calculating relevant thermodynamic parameters.

Because temperature did not change in a wide range under our experimental method, the enthalpy change could be considered to be a constant value. Thus, the thermodynamic parameters can be calculated by the van't Hoff equation

$$LnK=-\frac{\Delta H}{RT}+\frac{\Delta S}{R} \quad (3)$$

where $K$ is a binding constant at corresponding temperature, $\Delta H$ is the enthalpy change, $\Delta S$ is the entropy change, and $R$ is a gas constant. From the $LnK$ versus $1/T$ plot we can obtain the values of $\Delta H$ and $\Delta S$.

As known, the free energy change ($\Delta G$), enthalpy change ($\Delta H$) and entropy change ($\Delta S$) have the following relationship:

$$\Delta G=\Delta H-T\Delta S \quad (4)$$

From Eqs. (3) and (4), corresponding thermodynamic parameters was acquired, as shown in Table 1. It can be seen that all the free energies are about −26 kJ mol$^{-1}$, indicating that the binding process does not need extra addition of energy and can take place spontaneously. $\Delta H<0$ and $\Delta S>0$ mean that the electrostatic interactions may play a leading role in the 3d–HSA complex formation.

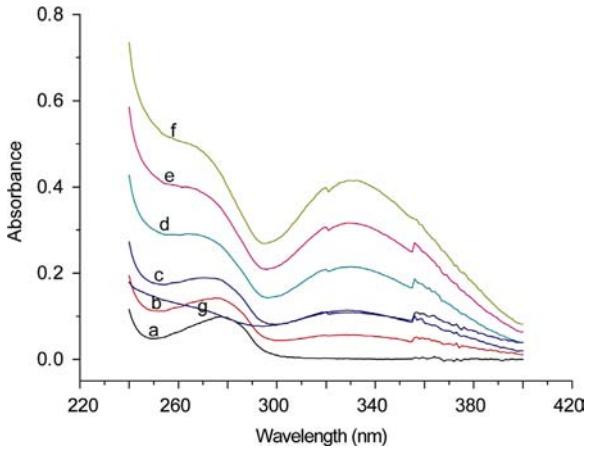


**Fig. 3.** UV–vis spectra of HSA in the absence (a) and presence (d–f) of 3d. The concentration of HSA was 2.5 μM; the molar ratios of HSA to 3d were 1:1 (b), 1:2 (c), 1:4 (d), 1:6 (e), and 1:8 (f). (g) 2.5 μM 3d only.

From fluorescence quenching results we know that 3d can bind to HSA spontaneously with relatively high association constant. This property endows 3d the capability that it can be deposited by HSA and be transferred to tumor in the circulatory system so as to produce antitumor action. This good property allows 3d move toward to being an efficient antitumor lead compound.

### 3.2. UV–vis absorption spectra analysis

UV–vis absorption spectroscopy is one of the most useful way to study conformational change of protein and detect complex formation [43]. From Fig. 3 we can see that the free HSA had an absorption peak at the wavelength of 280 nm, which is known as the absorption peak of tryptophan residues, tyrosine residues and phenylalanine residues. The absorption spectra intensities of HSA increased with the addition concentration of 3d, and the maximal peak had a blue-shift from 280 nm to 271 nm. As we all know, the absorption spectra have significant relationship with chromophores of protein. Chromophores exist in various microenvironment and it is determined by the conformation of whole protein. The conformational change of protein surely will alter the microenvironment and thus result in the change of ultraviolet absorption spectrum, and vice-versa. Therefore, the variation of UV–vis absorption spectra obviously demonstrated that 3d could bind to HSA and induce conformational change. These results are clearly in line with conclusion of the fluorescence spectra and confirmed its correctness.

### 3.3. CD spectra analysis

Generally, CD spectroscopy is popular in molecular biology area to study the spatial structure of proteins, especially secondary structure and changes of their conformation. Fig. 4 shows the CD

spectra of free HSA and HSA–3d complex. The CD spectra exhibited two negative bands at wavelengths of 208 nm and 222 nm. These two wavelength points are the characteristic peaks of α-helix structures and both of them can be used to calculate its content. Though the intensity of CD spectra decreased with increasing concentrations of the drug, the peaks did not shift apparently. These results were expressed as ellipticity (mdeg), which was obtained directly from the instrument. The secondary structure percentage of α-helix in HSA before and after interaction with 3d was determined by the following equations [44]:

$$[\theta]^{\mathrm{MRW}} = \frac{\mathrm{CD_{obs}}(m\mathrm{deg})}{C_{\mathrm{p}} n l \times 10} \tag{5}$$

$$\alpha - \mathrm{helix}(\%) = \frac{-[\theta]_{222}^{MRW} - 2324}{30300} \times 100\% \tag{6}$$

where $[\theta]^{MRW}$ is mean residue ellipticity (MRW), $CD_{obs}$ is observed ellipticity, $C_p$ is the molar concentration of the protein, $n$ is amino acid residues number, $l$ is the path length and $[\theta]_{222}^{MRW}$ is the MRW at wavelength of 222 nm. Calculated results showed that the percentage of α-helix decreased from 47.0% in pure HSA to 41.5% and 37.9% when molar ratios of 3d to HSA are 1:1 and 2:1, respectively. CD spectra explain the binding effect of HSA through quantitative analysis. It can provide the information that whether the drugs can interact with proteins and the degree of the interaction. This result indicated that the interaction between drug 3d and HSA led to a slight decrease in the helical structure content of protein [9]. Since we have already known that 3d induced HSA conformational change through UV–vis absorption spectra analysis, the decline of α-helix ratio may result from α-helix uncoiling because of the microenvironment change of HSA deduced by the conformational alteration.

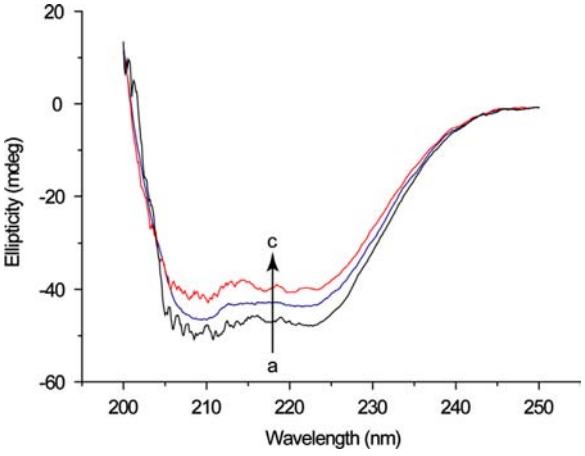


**Fig. 4.** CD spectra of the HSA–3d system in the presence of increasing concentrations of 3d in pH 7.4 phosphate buffer at 25 °C. The concentration of HSA was 5 μM; the molar ratios of HSA to 3d were 1:0 (a), 1:1 (b), and 1:2 (c).

### 3.4. Molecular modeling

Molecular modeling was employed to further understand the possible conformation of 3d–HSA complex. The interaction of warfarin with HSA was widely investigated as a model to study ligand/HSA interaction. Warfarin binds to HSA with high affinity in plasma and about 99% of warfarin formed complex with HSA, which has a correlationship with its high bioavailability. As shown in Fig. 5A, 3d, just as warfarin, could bind to HSA in the subdomain IIA which is a main binding domain and most ligands exhibit their unique biological activity by binding to this domain [32,33]. 3d was capable of exactly entering into this subdomain and forming some key non-covalent interactions with amino residuals around it (as shown in Fig. 5B). The specific interactions were as follows: (1) three hydrogen bonds, formed between C═O from urea bonding and $NH_2$ of ARG222, NH and $NH_2$ of ARG218. (2) three cation–π interactions, one formed between chlorobenzene ring and the ammonium cation of ARG218; the second appeared between C ring of flavones backbone and the ammonium cation of ARG222; the third existed between C ring of flavones backbone and the ammonium cation of LYS199. Molecular docking results showed that 3d could well fit into HSA subdomain IIA. As illustrated in well-known data, this subdomain plays the dominant role in drug deposition and delivery; the specific interactions between 3d and HSA reminded us that this compound could be transferred to target tissue or organ by HSA in the circulatory system. The docking study is in agreement with the above experimental data shown in this manuscript and this will supply us important information about pharmacological properties of 3d [10].

## 4. Conclusion

Although 3d was designed as an inhibitor of specific protein target of definite sites, the interaction of this molecule with nontarget protein like HSA is still useful in drug development. In the present work, the binding of 3d with HSA was investigated using multispectroscopic (such as fluorescence spectroscopy, circular dichroism spectroscopy and UV–vis spectroscopy) and molecular docking approach. The results indicated that the fluorescence of HSA was quenched by 3d in the mechanism of static quenching with association constant $5.26 \pm 0.04 \times 10^4\ \mathrm{L\ mol^{-1}}$ at 298 K. Through the calculated thermodynamic parameters, we presumed that the electrostatic interactions may feature the binding process and the progress could happen spontaneously. From the results of UV–vis and CD spectra it could be deduced that the conformation of 3d was changed when adding 3d to HSA. Moreover, molecular docking results suggested that 3d could bind to HSA into the

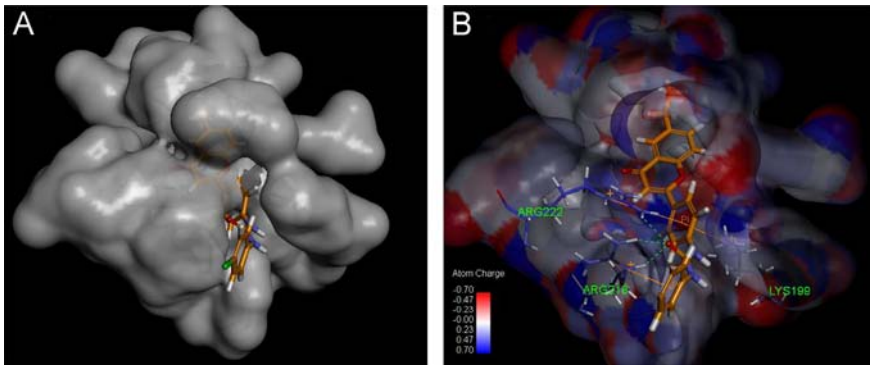


**Fig. 5.** Molecular docking of HSA with 3d. (A) 3d docked in the binding pocket of HSA. (B) The interaction mode between HSA and 3d.

hydrophobic cavity of subdomain IIA. The residuals ARG218, ARG222 and LYS199 formed corresponding interaction with 3d to participate in the stabilization of the 3d–HSA complex. In summary, 3d can bind to HSA in a relative stable way so that it can be transferred and deposited. The investigation of drug–protein interaction provides important information for drug screening at the early stage of drug development.

## Acknowledgment

This work was supported by China Ministry of Science and Technology under Contract No. 2012ZX09506001-010, the National High Technology Research and Development Program of China (863 Program) (No. 2013AA092902), the National Natural Science Foundation of China (Nos. 21272134 and 21172129) and the National Youth Science Foundation (No. 21305074).

## References

[1] A.Y. Khan, M. Hossain, G. Suresh Kumar, Chemosphere 87 (2012) 775–781.
[2] L.H. Lucas, K.E. Price, C.K. Larive, J. Am. Chem. Soc. 126 (2004) 14258–14266.
[3] A. Martincic, M. Cemazar, G. Sersa, V. Kovac, R. Milacic, J. Scancar, Talanta 116 (2013) 141–148.
[4] Y. Zhang, L. Dong, J. Li, X. Chen, Talanta 76 (2008) 246–253.
[5] D.C. Carter, J.X. Ho, Adv. Protein Chem. Struct. Biol. 45 (1994) 153–203.
[6] X. Pan, P. Qin, R. Liu, J. Wang, J. Agric. Food Chem. 59 (2011) 6650–6656.
[7] X.M. He, D.C. Carter, Nature 358 (1992) 209–215.
[8] S. Tabassum, W.M. Al-Asbahy, M. Afzal, F. Arjmand, J. Photochem. Photobiol. B: Biol. 114 (2012) 132–139.
[9] N. Shahabadi, A. Khorshidi, N.H. Moghadam, Spectrochim. Acta Part A: Mol. Biomol. Spectrosc. 114 (2013) 627–632.
[10] S.R. Feroz, S.B. Mohamad, N. Bujang, S.N. Malek, S. Tayyab, J. Agric. Food Chem. 60 (2012) 5899–5908.
[11] T. Peters Jr., Adv. Protein Chem. Struct. Biol. 37 (1985) 161–245.
[12] U. Kragh-Hansen, V.T. Chuang, M. Otagiri, Biol. Pharm. Bull. 25 (2002) 695–704.
[13] C. Andre, A. Xicluna, J.F. Robert, M. Thomassin, Y.C. Guillaume, Talanta 65 (2005) 814–818.
[14] J. Ma, Y.M. Yin, H.L. Liu, M.X. Xie, Curr. Org. Chem. 15 (2011) 2627–2640.
[15] C.S. Buer, N. Imin, M.A. Djordjevic, J. Integr. Plant Biol. 52 (2010) 98–111.
[16] S. Zhang, L. Zheng, D. Dong, L. Xu, L. Yin, Y. Qi, X. Han, Y. Lin, K. Liu, J. Peng, Food Chem. 141 (2013) 2108–2116.
[17] Y. Rong, Z. Wang, J. Wu, B. Zhao, Spectrochim. Acta Part A: Mol. Biomol. Spectrosc. 93 (2012) 235–239.
[18] K. Sadasivam, R. Kumaresan, Spectrochim. Acta Part A: Mol. Biomol. Spectrosc. 79 (2011) 282–293.
[19] C. Wan, M. Cui, F. Song, Z. Liu, S. Liu, Int. J. Mass Spectrom. 283 (2009) 48–55.
[20] Y.-Y. Li, Q.-F. Zhang, H. Sun, N.-K. Cheung, H.-Y. Cheung, Talanta 105 (2013) 393–402.
[21] L.N. Francescato, S.L. Debenedetti, T.G. Schwanz, V.L. Bassani, A.T. Henriques, Talanta 105 (2013) 192–203.
[22] J. Cao, W.-L. Dun, Talanta 84 (2011) 155–159.
[23] M.G. Hertog, E.J. Feskens, P.C. Hollman, M.B. Katan, D. Kromhout, Nutr. Cancer 22 (1994) 175–184.
[24] H.P. Kim, I. Mani, L. Iversen, V.A. Ziboh, Prostaglandins Leukot. Essent. Fatty Acids 58 (1998) 17–24.
[25] D. Gao, F. Jin, H. Liu, Y. Wang, Y. Jiang, Talanta 118 (2014) 382–388.
[26] I. Lammers, V. Lhiaubet-Vallet, F. Ariese, M.A. Miranda, C. Gooijer, Spectrochim. Acta Part A: Mol. Biomol. Spectrosc. 105 (2013) 67–73.
[27] K.M. Duffell, S.A. Hudson, K.J. McLean, A.W. Munro, C. Abell, D. Matak-Vinkovic, Anal. Chem. 85 (2013) 5707–5714.
[28] M.L. D'Alessandro, D.A. Ellis, J.A. Carter, N.L. Stock, R.E. March, Int. J. Mass Spectrom. 345–347 (2013) 28–36.
[29] R. Haselberg, S. Harmsen, M.E. Dolman, G.J. de Jong, R.J. Kok, G.W. Somsen, Anal. Chim. Acta 698 (2011) 77–83.
[30] H. Wan, A. Ostlund, S. Jonsson, W. Lindberg, Rapid Commun. Mass Spectrom. 19 (2005) 1603–1610.
[31] J. Sun, B. He, Q. Liu, T. Ruan, G. Jiang, Talanta 93 (2012) 239–244.
[32] Y. Zhang, S. Shi, J. Guo, Q. You, D. Feng, J. Chromatogr. A 1293 (2013) 92–99.
[33] W. Wang, W. Zhang, Y. Duan, Y. Jiang, L. Zhang, B. Zhao, P. Tu, Spectrochim. Acta Part A: Mol. Biomol. Spectrosc. 115 (2013) 57–63.
[34] M.B. Gholivand, A.R. Jalalvand, H.C. Goicoechea, M. Omidi, Spectrochim. Acta Part A: Mol. Biomol. Spectrosc. 115 (2013) 516–527.
[35] X. Wang, Y. Liu, H. Wang, Talanta 116 (2013) 368–375.
[36] J. Ghuman, P.A. Zunszain, I. Petitpas, A.A. Bhattacharya, M. Otagiri, S. Curry, J. Mol. Biol. 353 (2005) 38–52.
[37] C. Qin, M.X. Xie, Y. Liu, Biomacromolecules 8 (2007) 2182–2189.
[38] A. Sulkowska, J. Mol. Struct. 614 (2002) 227–232.
[39] G. Wang Zhang, L. Pan, J. Agric. Food Chem. 60 (2012) 2721–2729.
[40] Y.J. Hu, H.G. Yu, J.X. Dong, X. Yang, Y. Liu, Spectrochim. Acta Part A: Mol. Biomol. Spectrosc. 65 (2006) 988–992.
[41] C.B. Murphy, Y. Zhang, T. Troxler, V. Ferry, J.J. Martin, W.E. Jones, J. Phys. Chem. B 108 (2004) 1537–1543.
[42] L. Soltes, M. Mach, J. Chromatogr. B 768 (2002) 113–119.
[43] Y.H. Chen, J.T. Yang, H.M. Martinez, Biochemistry 11 (1972) 4120–4131.
[44] Z. Cheng, Y. Zhang, J. Mol. Struct. 879 (2008) 81–87.